Opposition Control of Near-wall Turbulence – A Real-time Experiment

Henry Rebbeck
Flexifoil International
27 Regal Drive, Soham, Cambridge CB7 5BE, UK
henry@flexifoil.com

Kwing-So Choi
School of Mechanical, Materials, Manufacturing Engineering and Management
University of Nottingham
University Park, Nottingham NG7 2RD, UK
kwing-so.choi@nottingham.ac.uk

ABSTRACT

Recent DNS studies have shown that the near-wall turbulence can be controlled with a simple control scheme, providing up to 25% skin-friction drag reduction. Opposition control establishes a 'virtual wall', a plane with effectively no through flow, preventing a downwash of high-momentum fluid towards the wall during the sweep events. In this paper, we report recent experimental results where opposition control was carried out in *real time* using wall-normal jet from an actuator. By improving on the detection technique and the actuator used, we were able to selectively cancel the downwash of high-momentum fluid in the near-wall region of the turbulent boundary layer.

INTRODUCTION

Recent studies using Direct Numerical Simulations have shown that the near-wall turbulence of the boundary layer can be controlled with a relatively simple control scheme. For example, Choi *et al.* (1994) used blowing and suction at the wall, in opposition to the wall-normal fluid velocity at a small distance from the wall, providing up to 25% drag reduction. Opposition control establishes a 'virtual wall' (Hammond *et al.*, 1998), a plane with effectively no through flow, halfway between the detection point and the wall, preventing a downwash of high-momentum fluid towards the wall during the sweep events.

Moving a Gaussian bump on one of the turbulent channel walls, Carlson and Lumley (1996) conducted a DNS study for a possibility of reducing skin-friction drag. When the high-speed streaks are lifted by the bump, the adjacent low-speed region was expanded resulting in a drag reduction. When the bump lifted the low-speed streaks, on the other hand, drag increase was observed as the adjacent high-speed region is expanded. Endo *et al.* (2000) carried out a similar DNS study in a channel flow, where a feedback control of near-wall turbulence was conducted. Another study was conducted by Kang and Choi (2000), who attempted to obtain turbulent drag reduction by locally deforming the wall in a channel flow based on control strategies previously proposed.

Rathnasingham and Breuer (1997) used piezo-electric resonant actuators in their experiment to suppress large-scale coherent motions of the boundary layer using wall-normal jets. A linear transfer function between detector sensors and actuators was obtained first, and an adaptive feed-forward control was applied to the flow to minimise the turbulence intensity downstream of the actuators. The control algorithm worked well without detecting specific near-wall structures in the turbulent boundary layer. These are realistic in terms of strategy implementation for drag reduction, but they lacked a physical explanation for the mechanisms of drag reduction using actuators.

First experimental study of opposition control of near-wall turbulence was carried out by Rebbeck and Choi (2001) using a wall-normal jet from a piston-type actuator, where selective cancelling of the downwash of high-momentum fluid was carried out during the sweep events. By employing an innovative methodology they were able to study the effectiveness of the scheme without carrying out real-time control, overcoming experimental difficulties associated with the high frequency responses required for the turbulence control. Here, the actuator was operated at a fixed cycle of 1 Hz, and velocity signals from the detector and hot-wire sensor downstream of the actuator were simultaneously sampled. They were then analysed off line to obtain an ensemble-averaged burst signature during the sweep events when they are opposed by a wall-normal jet. This method demanded a large amount of data to provide enough hits with the sweep events by the wall-normal jet. About one million sets of data were collected altogether at a sampling speed of 1 kHz during the experiment. Obviously, the amount of data required depends on the window width of the targeted events. For each window of $t^+ = tu^{*2}/\nu = 2.2$, where t is the time, there were more than 25 hits, from which an ensemble-averaged burst signature of the modified sweep events was obtained.

The motivation of the present study is to extend this study of off-line control of near-wall turbulence to *real-time*. In doing so, we were able to investigate how the near-wall turbulence structure of the boundary layer is modified when opposition control is applied to individual sweep events. At the same time, we could assess a feasibility of opposition control of the near-wall turbulence in obtaining skin-friction drag reduction. In this paper, we describe the process in which real-time control was made possible, showing the modification made to the near-wall structure during the sweep events when the downwash of high momentum fluid was selectively cancelled by the wall-normal jet.

Table 1: Boundary-layer parameters.

δ(m)	θ(m)	H	U (m/s)	u^* (m/s)	Re_θ
0.0084	0.0059	1.43	2.0	0.0907	786

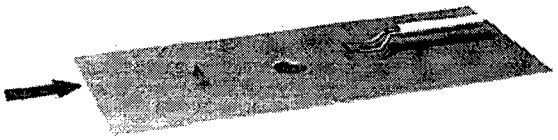

Figure 1: Schematic diagram of test configuration showing the detector (left), actuator (centre) and sensor (right).

EXPERIMENTS

Experiments were carried out in a closed-return wind tunnel, where a turbulent boundary layer was developed over a flat plate with zero pressure gradient. The boundary-layer parameters for the experiment are shown in Table 1, where δ is the boundary-layer thickness, θ the momentum thickness and H the shape factor. A trip device was placed at 100 mm from the leading edge of the test plate. The mean velocity profile obtained at the measurement location in the test section had nearly a decade-wide logarithmic region. In addition, all the higher turbulence statistics including the RMS intensity, skewness and kurtosis of u-velocity fluctuation showed standard profiles typical of a fully developed turbulent boundary layer.

Figure 1 is a schematic diagram of test configuration showing the detector, actuator and downstream sensor. The detector was made of a single hot-wire probe of 5 μm diameter and 1.0 mm sensing length, mounted on the test surface from below at $y^+ = 8$. Only the sensor and prong portion of the hot-wire probe were exposed to the flow in order to minimise aerodynamic interference with the probe body. We have adopted a loud speaker with a 1mm diameter ($d^+ = 10$) nozzle as an actuator for real-time control, with which we can control the strength and duration of the wall-normal jet from the wall surface. The nozzle was located at 1.20 m from the leading edge of the test plate, $x^+ = 72.5$ downstream of the detector. The velocity field downstream of the actuator was measured by a Dantec 55P15 boundary-layer type hot-wire probe mounted on a three-dimensional traverse gear. Velocities from the anemometer and the timing signal of the actuator were simultaneously sampled and they were converted to digital format using an Iotech ADC488/8SA A/D converter for later analysis. The sweep events were detected when the positive gradient of the u-component velocity from the detector exceeded a preset threshold.

RESULTS

The time available for carrying out real-time control is generally determined by the distance between the detector and the actuator and the convection velocity of the turbulence structure, which is about $u_c^+ = 14$ within the near-wall region of the turbulent boundary layer (Rebbeck 2002). However, it also depends on the wall normal position of the detector h_d^+ relative to the virtual wall height h_v^+, through the following relationship.

$$t^+ = x^+/u_c^+ - (h_v^+ - h_d^+) / \tan\theta\, u_c^+$$

where, θ is the shear-layer front angle in the turbulent boundary layer. In the present experiment, this amounts to $t^+ \approx 5$ ($t \approx 8$ ms), suggesting that neither the detection method nor the actuator that has been used in the previous study (Rebbeck and Choi, 2001) is fast enough. Therefore, alternative techniques need to be investigated for real-time control.

The most common method used for detecting near-wall structures is the VITA method, which can locate rapidly changing signals that characterise coherent structures. Since the VITA method requires a computation of running variance within a window of typically $t^+ = 10$ (equivalent to $t = 16$ms in our experiment), and comparison with a preset threshold value (typically $k = 1$), the decision could not be made at least for $t^+ = 5$ (or $t = 8$ms) after the event. This is such a large overhead in real-time control, which led us to use the gradient method of detecting the sweep events. Before implementing the new method of detecting the sweep events, the number of events detected by the gradient method was compared to that by the VITA method. Here, actual threshold value for the gradient method is somewhat arbitrary, depending on the r.m.s. velocity fluctuation level. Figure 2 shows the signature of the VITA event compared with that obtained by the gradient method which produced 393 hits in a 100 second period. This compares with a 132 hits by the VITA method, in which 98 events were also detected by the gradient method. It suggests that the sweep signature detected by the gradient method is slightly shorter in both duration and magnitude than that detected by the VITA event, probably due to the high number of detections. When the threshold value was set to a high enough value, the gradient detection technique detected essentially the same events therefore the signature as those by the VITA method (Rebbeck, 2002).

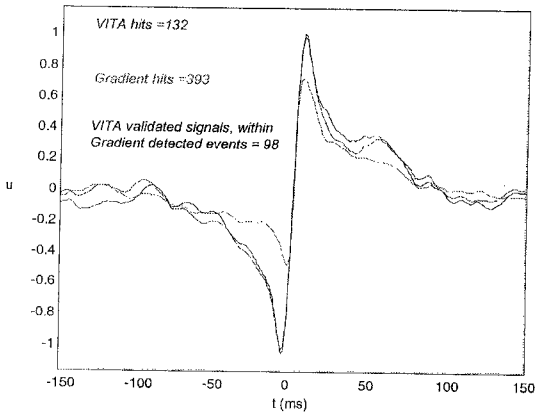

Figure 2: Comparison of the sweep signature detected by the VITA method with that by the gradient method.

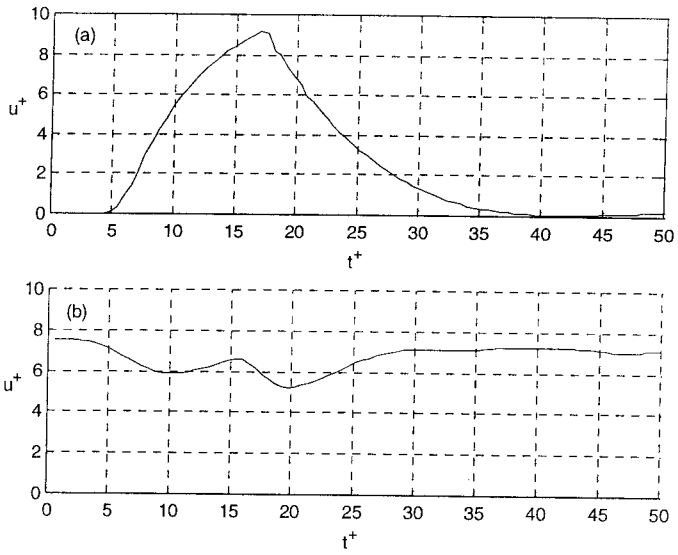

Figure 4: Velocity profiles at $y^+ = 7.5$ above the loudspeaker actuator for the still conditions (a) and in the turbulent boundary layer (b) when driven for 25ms ($t^+ = 14$) duration by a 15V square wave.

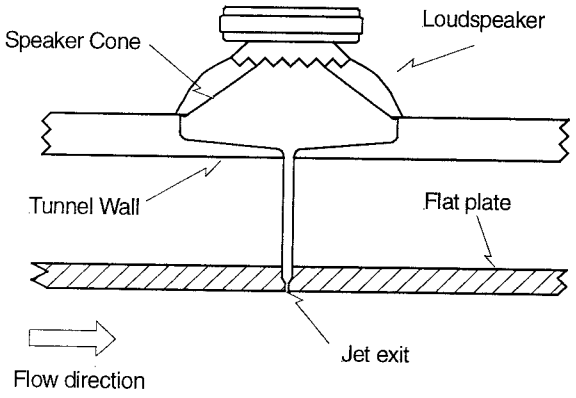

Figure 3: Diagram of loudspeaker mounting and creation of wall normal jet.

Figure 5 shows the development of low-speed region in the near-wall region of the turbulent boundary layer, which was created by the wall-normal jet from the actuator. Opposition control of near-wall turbulence would work by cancelling the high-speed flow region during the sweep events by the low-speed region created by the wall-normal jet from the actuator.

The piston-type actuator that we have successfully used in the previous *off-line* investigation was driven by solenoid with a typical response time of $t^+ = 20$ (or $t = 40$ms). In comparison, the loudspeaker actuator (see Fig. 3) that we have implemented in the present study has much shorter response time of $t^+ \approx 3$.

The square-wave input to the loudspeaker was adjusted to give a similar output by the piston-type actuator used in the previous study (Rebbeck and Choi, 2001). Figure 4(a) shows that the peak velocity of the wall-normal jet has a similar value of $v^+ = 9$, but it has a slightly increased duration of $t^+ = 14$ as compared to the piston-type actuator. When the wall-normal jet was issued into the turbulent boundary layer (see Fig. 4(b)), the low u-velocity profile had a characteristic "w" shape (Rebbeck and Choi, 2001).

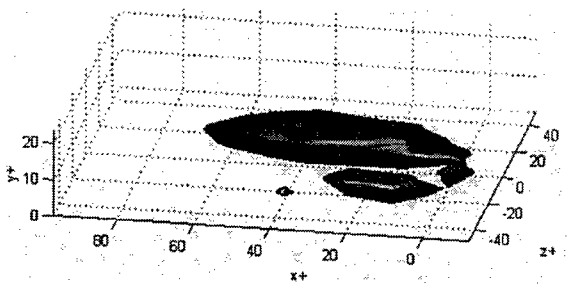

Figure 5: The development of the flow field downstream of the actuator, showing the low-speed region (blue = -0.75 u^+) and high-speed region (red = 0.25 u^+).

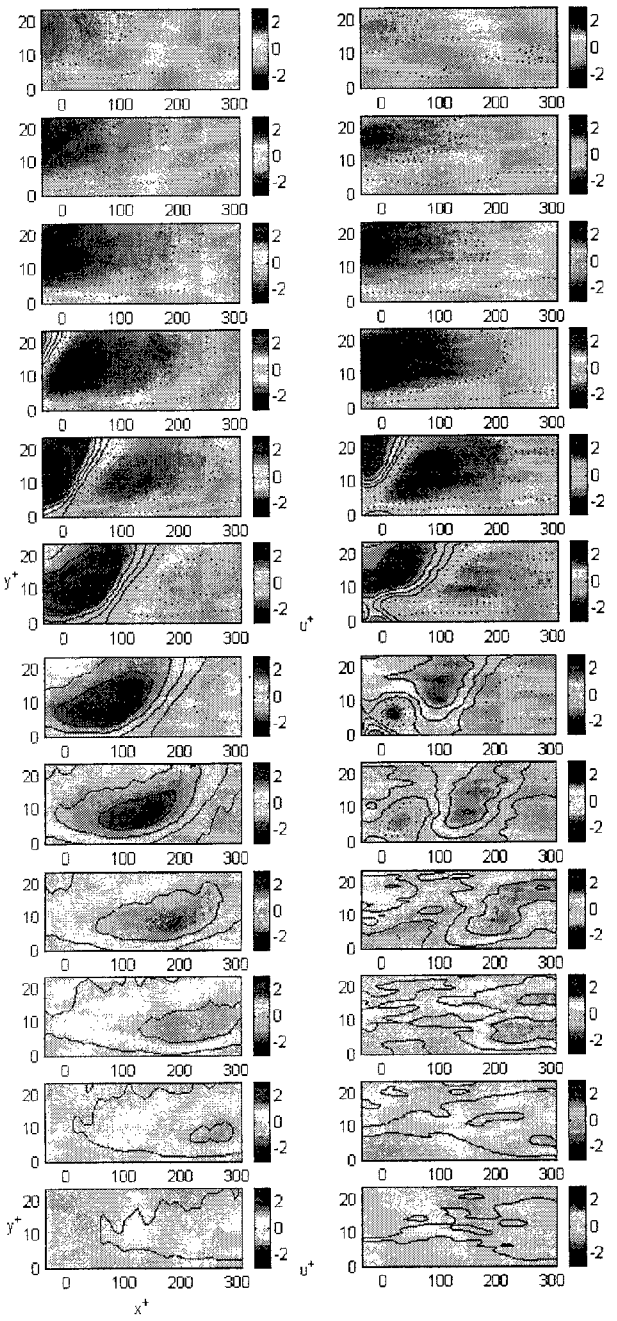

Figure 6: Evolution of the sweep event with actuation (right) and without (left). The figure shows the ensemble averaged u-component velocity in the x-y plane. Contour intervals of 0.5 u^+ are shown, with dotted contours corresponding to negative velocity (less than the mean). Time increment is t^+ = 5.5 between each figure.

The u-component velocity in x-y plane along the centre line of measurement from x^+ = –50 to 300 and y^+ = 0 to 22 is shown in Fig. 6. The wall-normal jet from the actuator is seen to have an impact on the sweep event from the fifth plot of the figure onwards. It is shown that the jet deflects the high-speed front away from the wall, reducing the high u-fluctuation velocity in the near wall region. The peak velocity seen at y^+ = 8 to 13 during the sweep is clearly reduced. Beyond the region of x^+ = 100 in the downstream, however, the effect is less marked as the sweep appears to have advanced closer to the wall, increasing the near-wall velocity gradient and hence increased skin friction. The magnitude the increase is still less than that of the unmodified flow.

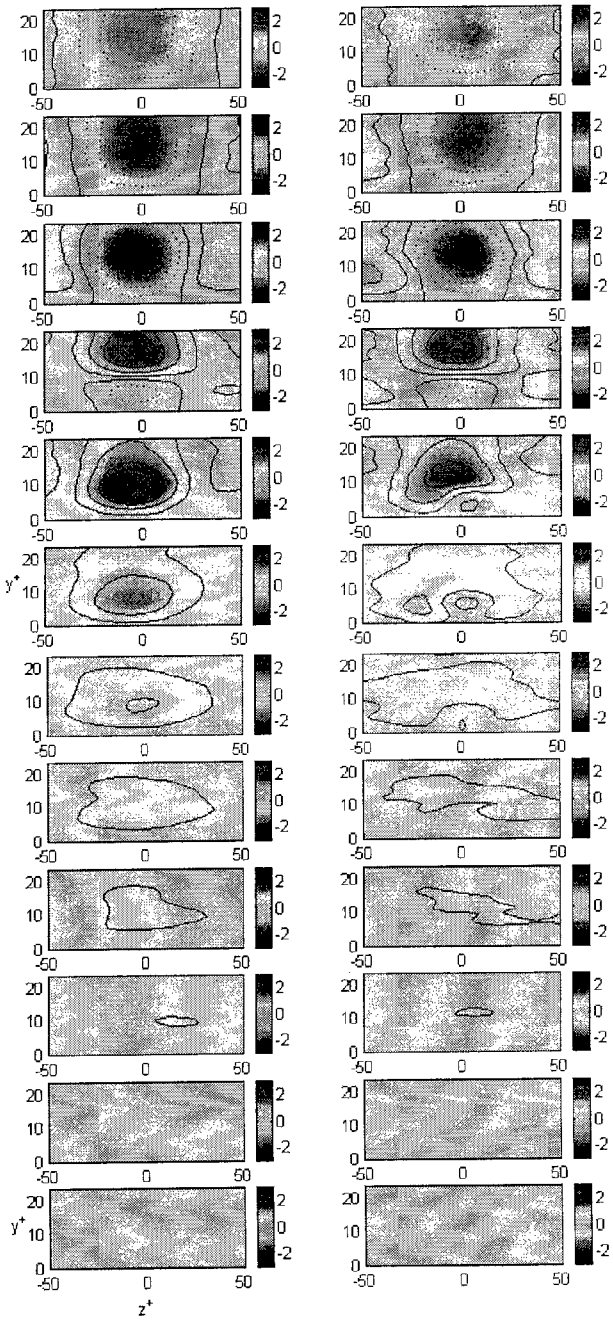

Figure 7: Evolution of the sweep event with actuation (right) and without actuation (left), showing the ensemble averaged u-component velocity in the y-z plane at x^+ = 14 downstream of the actuator.

The change in the turbulent flow structure in y-z plane (Fig. 7) clearly shows the opposition action against the downwash of high-speed flow during the sweep event. The high-speed region is initially countered by the wall-normal jet, but eventually some of the high velocity fluid moves around the sides of the jet to impinge on the wall. This is clearly due to the mismatch of the size of the wall-normal jet to that of the downwash. However, the speed of the downwash as well as the area of impingement was significantly reduced, indicating a possible drag reduction by opposition control.

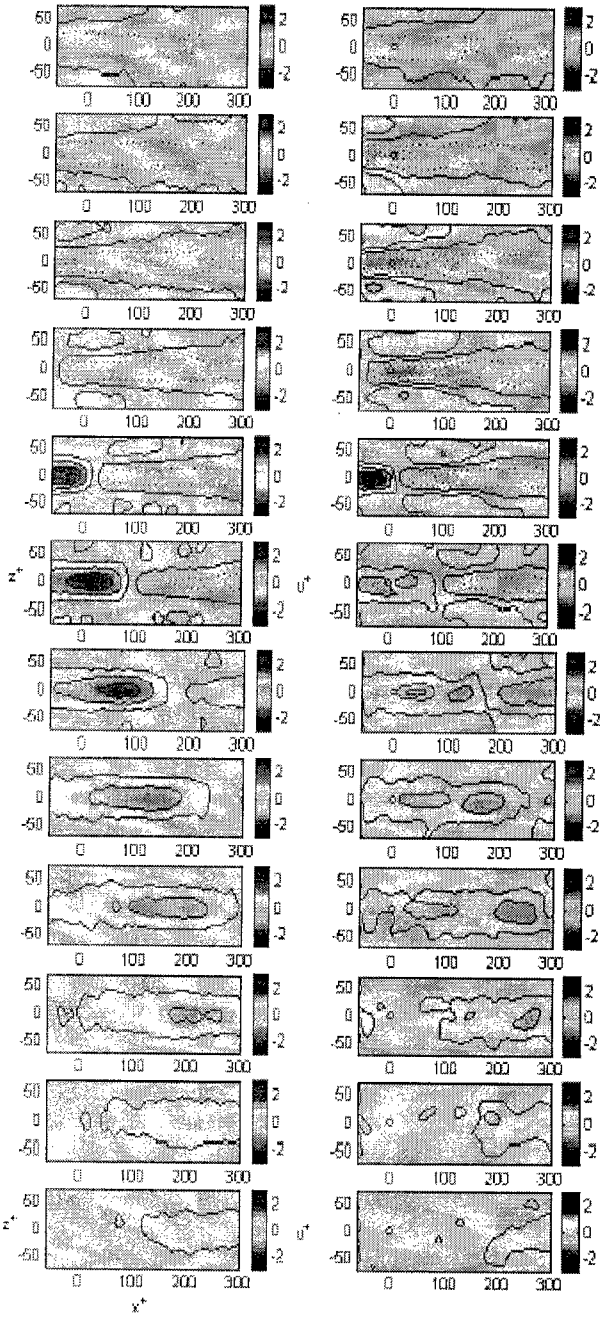

Figure 8: Evolution of the sweep event with actuation (right) and without actuation (left), showing the ensemble averaged u-component velocity in the x-z plane at $x^+ = 14$ downstream of the actuator.

The development of the u-component velocity in x-z plane is shown in Fig. 8 when real-time control was applied. The jet was issued into the boundary layer at location of $x^+ = 0$, $z^+ = 0$ and its effect can first be observed in the 6th plot, where a high speed sweep event is modified by a central well of low-speed fluid created by the wall normal jet. Subsequent plots show that the sweep is being destroyed by the jet.

Interestingly the propagation speed of the sweep event appeared faster than that of the low speed fluid created by the actuator, as shown in Fig. 9. The sweep event moves with a convection velocity of $u^+ = 12$~14, whereas the low speed region created by the wall normal jet seems to advance at a speed closer to the local mean velocity of the boundary layer. This implies that the actuator should be much longer in the streamwise direction to be more effective in cancelling the sweep events. Indeed, Rathnasingham and Breuer (1997) used an actuator with a streamwise length of $x^+ = 150$, and Endo *et al.* (2000) had utilised actuators with $x^+ = 172$ in their DNS simulation. Alternatively, we should have a series of orifices separated by approximately $x^+ = 80$ to 100 in the streamwise direction, and they can be operated with a short time delay between them.

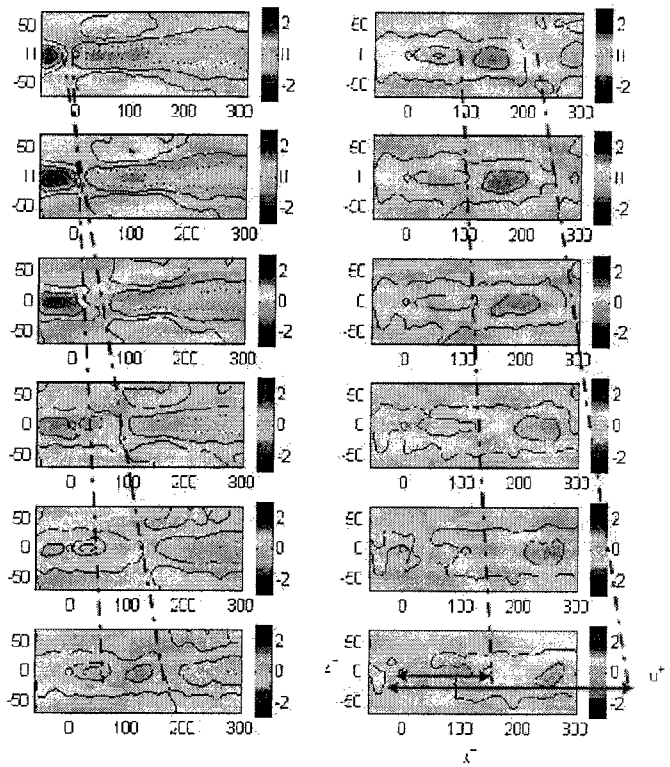

Figure 9: The propagation of the sweep event and the low speed region from the wall normal jet in the x-z plane. Plots have time increments of 5ms ($t^+ = 5.5$) between each figure with the time sequence from top left to bottom left then continuing from top right to bottom right. A circle at the origin of the individual plots indicates the actuators size and position. The blue line (left) indicates progression of the low velocity region produced by the wall normal jet, and the red line (right) indicates the progression of the sweep event. The sweep travels roughly by $x^+ = 420$ in the 55ms ($t^+ = 30$) period and the low-speed region by $x^+ = 180$ within the same period. Arrows indicate the distances travelled.

CONCLUSIONS

Choi *et al.* (1994) and Hammond *et al.* (1998) showed in their DNS study that opposition control can produce up to 25% drag reduction, providing that the virtual wall can be created within the viscous sublayer (y^+ = 5 to 7.5). Our experimental results from this study provides further evidence to their work for the importance of the virtual wall and its effectiveness in opposition control.

Figure 10(a) shows the near-wall flow structure in the y-z plane at the instant when the sweep event impinged on the wall. Arrows show the direction of movement of the high-speed region during the downwash. Figure 9(b) shows the sweep event in the same instant when it was opposed by the wall-normal jet from the actuator. The actuator inhibits the downwash of the high-speed fluid by establishing the virtual wall, at $y^+ \approx 12$. It is not as an effective a barrier as that of Hammond *et al.* (1998), as some part of the downwash was not stopped completely by opposition control. However, the control jet deflects the sweep event in spanwise direction, reducing the impact of the downwash fluid impacting on the wall.

It has been suggested by Choi *et al.* (1994) that the regeneration mechanism within the turbulent boundary layer can be eventually suppressed by deterring the sweep events, leading to skin-friction reduction. Similar argument has been put forward by Choi (1996). This provides hope for skin-friction drag reduction by using opposition control, where we have demonstrated the ability in combating with the sweep events. Indeed, our results at t^+ = 33 (equivalent to x^+ = 462 in the downstream of the actuator) show considerable break up of the coherence of the near-wall turbulence structures, indicating a reduction in the regeneration process within the turbulent boundary layer.

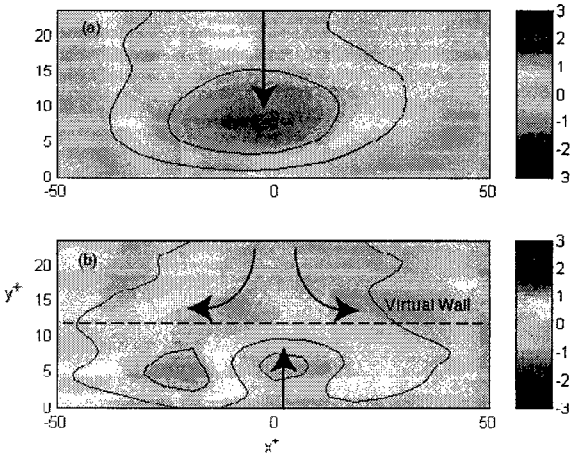

Figure 10: Ensemble averaged u-component velocity in the y-z plane located at x^+ = 14 downstream from the actuator. Plot (a) shows the unmodified case and plot (b) modified by the actuator.

ACKNOWLEDGEMENTS

The authors acknowledge the support received from the Leverhulme Trust and the University of Nottingham during the course this investigation.

REFERENCES

Carlson, H. A., and Lumley, J. L., 1996, "Active Control in the Turbulent Wall Layer of a Minimal Flow Unit," *J. Fluid Mech.*, 329, 341.

Choi, K.-S., 1996, "Turbulent Drag Reduction Strategies," in *Emerging Techniques in Drag Reduction*, eds. by K.-S. Choi *et al.*, MEP, London, pp. 77-98.

Choi, H., Moin, P., and Kim, J., 1994, "Active Turbulence Control for Drag Reduction," *J. Fluid Mech.*, 262, 75.

Endo, T., Kasagi, N., and Suzuki, Y., 2000, "Feedback Control of Wall Turbulence with Wall Deformation," *Int. J. Heat and Fluid Flow*, 21, 568.

Hammond, E. P., Bewley, T. R., and Moin, P., 1998, "Observed Mechanisms for Turbulence Attenuation and Enhancement in Opposition-controlled Wall Bounded Flows," *Phys. Fluids*, 10(9), 2421.

Kang, S., and Choi, H., 2000, "Active Wall Motions for Skin Friction Drag Reduction," *Phys. Fluids*, 12(12), 3301.

Rathnasingham, R., and Breuer, K. S., 1997, "System Identification and Control of a Turbulent Boundary Layer," *Phys. Fluids*, 9(7), 1867.

Rebbeck, H., 2002, "Modification of the Near Wall Structure of a Turbulent Boundary layer by Opposition Control," PhD Thesis, University of Nottingham, UK.

Rebbeck, H., and Choi, K.-S., 2001, "Opposition Control of Near-wall Turbulence with a Piston-type Actuator," *Phys. Fluids*, 13(8), 2142.